Acoustic attenuation and optical-absorption effects on light scattering by acoustic phonons in superlattices

J. He, J. Sapriel, and R. Azoulay
Centre National d'Etudes des Télécommunications, 196 avenue Henri Ravera, 92220 Bagneux, France
(Received 3 January 1989)

The effects of acoustical attenuation and optical absorption on light scattering by acoustic phonons propagating along the superlattice axis are theoretically analyzed and experimentally probed in GaAs/AlAs and $Si/Si_{0.5}Ge_{0.5}$ superlattices. It is shown that the linewidth of the acoustic modes undergoes a clear narrowing near the Brillouin-zone edge due to the decrease of the group velocity of the phonons. It is also demonstrated that the damping of the acoustic waves makes the high-frequency modes at the Brillouin-zone edge shift into the "forbidden gaps" which have been evidenced in the case of lossless media. We have observed such a shift in a $Si/Si_{0.5}Ge_{0.5}$ superlattice sample at phonon energies around 14 cm^{-1} for which the acoustic attenuation can no longer be neglected. It is also shown that the effects of optical absorption on the relative intensity of the folded acoustic modes are particularly sensitive in the condition where the incident light is Bragg reflected by the interfaces. This intensity behavior has been observed in a GaAs/AlAs superlattice and agrees with the theoretical analysis.

I. INTRODUCTION

Raman scattering is a useful and versatile technique for the characterization of semiconductor superlattices. A great deal of information concerning the alternating-layer properties and the superlattice structure and quality can be obtained from the frequencies, linewidths, and relative intensities of the Raman phonon lines[1] and many Raman studies have been reported in different superlattice systems.[2–18]

The folding effect, due to the artificial period D of the superlattice along its growth axis, gives rise to additional photon branches separated by energy gaps. The frequencies of the folded acoustic modes have been well accounted for by both the elastic continuum[19,20] and linear chain models.[20,21] As to the relative intensities of the longitudinal acoustic mode (LA or Brillouin mode) and the folded longitudinal acoustic modes (FLA), a good agreement between theory and experiments has been obtained for a wide range of scattering wave vectors q by a recent model in which the scattered electromagnetic field is strictly calculated from Maxwell's equations and boundary continuity conditions.[22] (The scattering wave vector q is defined as the change of light-wave vector in the scattering process. In the backscattering geometry used in most experiments, q is twice the wave vector of the incident light.)

All previous models concerning the FLA frequencies and intensities have ignored the effects of the acoustic attenuation and optical absorption. Indeed these effects can be neglected as far as one considers scattering wave vectors q not too close to the Brillouin-zone edges ($q=\pi/D, 2\pi/D, \ldots$). Actually most of the previous experiments have been performed with q away from these values. In this paper we particularly focus on the scattering wave vectors ranging around π/D, which corresponds to Bragg reflection for the acoustic phonons, and near $2\pi/D$, where Bragg reflection occurs for both acoustic and light waves. In these critical regions one can expect an enhancement of the effects of the acoustic attenuation and optical absorption since both of them significantly change the Bragg reflections.

As in any other medium, the damping of the light and acoustic waves in the superlattice induces a broadening of the peaks in the light scattering spectra. This broadening effect has been analyzed by considering the superlattice as an effective medium in Refs. 9 and 14. Such an approximation is valid only for scattering wave vectors far from the critical values $0, \pi/D, 2\pi/D, \ldots$, as shown in this paper by using a more strict treatment. In addition, due to the acoustic and optical damping, a partial loss of the translational symmetry D of the wave functions along the growth axis occurs. This must affect the phonon dispersion curve and the intensity of the light scattered by these phonons. In this paper we consider the coefficients of optical absorption and acoustic attenuation not too large ($<1/D$) so that the waves can sweep several superlattice unit cells, otherwise the superlattice notion would be meaningless. Two kinds of superlattices were available for our experimental investigations: $Si/Si_{1-x}Ge_x$ and GaAs/AlAs superlattices oriented along [001]. Their periods were chosen in order to allow the study of the scattering wave vectors ranging around $q=\pi/D$ and $q=2\pi/D$, respectively.

In this study we follow the general treatment used in Ref. 22 for the intensity calculation and adapt it to the case where the acoustic attenuation and optical absorption are considered. The notations are essentially the same as used in this reference. The normalized frequencies Ω ($\Omega=\omega D/2\pi C$, C being the light velocity in vacuum) of the excited phonon modes as a function of the reduced scattering wave vector Q ($Q=qD/\pi$) are reproduced in Fig. 1, and the different branches FLA_m are indicated in different Brillouin zones (Q ranges between

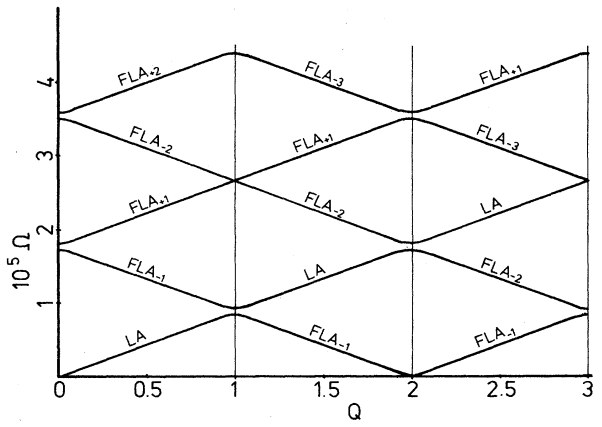

FIG. 1. Frequencies of the excited phonon branches as a function of the reduced scattering wave vector ($Q=qD/\pi$). The indexes m of the FLA_m are indicated according to Ref. 22.

0–1, 1–2, 2–3, . . .). For each FLA_m one has approximately the relation

$$\Omega=\frac{V}{C}|Q/2+m| \ . \tag{1}$$

Here V is the mean acoustic velocity ($V/D=d_1/v_1+d_2/v_2$), and m is the label associated with the folded longitudinal acoustic branch; $m=0$ corresponds to the direct acoustic mode (Brillouin line) whose frequency is essentially independent on the superlattice periods. For $q>\pi/D$ one can find folded acoustic modes at frequencies lower than the Brillouin mode.[16]

This paper is divided into five sections. In Sec. II we calculate the phonon dispersion curve and the acoustic attenuation as a function of the phonon energy in the case of acoustically absorbing superlattice layers. The experimental determination of the acoustic mode frequencies on a $Si/Si_{0.5}Ge_{0.5}$ superlattice near the Brillouin-zone edge are compared to the theoretical calculations. In Sec. III a study is performed of the broadening of the phonon modes by acoustical attenuation and optical absorption, and a parallel is made with the situation in homogeneous media. The effects induced by the optical absorption on the relative intensities of the phonon modes are depicted in Sec. IV with experiments in a long-period GaAs/AlAs superlattice ($qD\approx 2\pi$). A brief conclusion (Sec. V) summarizes the whole set of the results obtained here.

II. EFFECT OF THE ACOUSTIC ATTENUATION ON THE PHONON DISPERSION CURVES

For superlattices with a sufficient number of monolayers in the unit cell, the elastic continuum model can be applied to determine the acoustic behavior of the system. Because of the periodical modulation of the acoustic properties in the superlattice, the elastic wave which describes the propagation of the acoustic phonons along the superlattice axis is a Bloch function. In the case of acoustically nonabsorbing media, the wave vector K and the frequency ω of the phonon in the superlattice are related by the dispersion relation[19]

$$\cos KD=\cos k_1 d_1 \cos k_2 d_2-\frac{1}{2}\left[Z+\frac{1}{Z}\right]\sin k_1 d_1 \sin k_2 d_2 \ , \tag{2}$$

where $k_1=\omega/v_1$, $k_2=\omega/v_2$, and $Z=\rho_2 v_2/\rho_1 v_1$; ρ,v,d are, respectively, the mass density, acoustic velocity, and layer thickness, with subscripts 1 and 2 referring to the first or second layer in the superlattice unit cell. The period of the superlattice is then $D=d_1+d_2$. One of the characteristics of the acoustic phonon dispersion curves in lossless superlattices is the existence of the energy gaps, or stop bands at the Brillouin-zone edges. In these gaps, the wave vector K is complex ($K=k+i\alpha$) and the real part corresponds to $k=\pi/D, 2\pi/D$, etc. The acoustic wave is evanescent, and one can consider that it un-

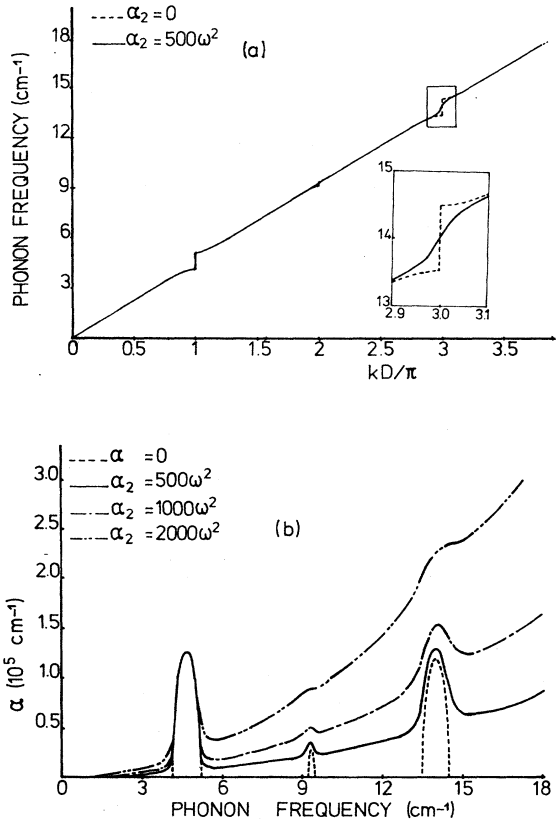

FIG. 2. Calculated dispersion curve (a) and attenuation-frequency relation (b) of the acoustic phonons in the Si-$Si_{0.5}Ge_{0.5}$ superlattice ($d_1=d_2=140$ Å). The increase of the attenuation at high frequency changes markedly the feature of the gap at $k=3\pi/D$ [see the inset of Fig. 1(a)]. We have used $\rho_1=2.33$ g/cm^3, $\rho_2=3.83$ g/cm^3, $v_1=8433$ m/s, $v_2=7330$ m/s, with subscripts 1 and 2 referring to Si and $Si_{0.5}Ge_{0.5}$, respectively. As to the acoustic attenuation, we have used $\alpha_1=0$, $\alpha_2=A\omega^2$ with different A values indicated in the figure (α,ω are expressed in cm^{-1}).

dergoes an attenuation in the direction of the propagation. These gaps have been evidenced either by Raman scattering[5,8] or by phonon-transmission experiments[23–25] for low-frequency phonons or in superlattices consisting of crystals with small acoustic attenuation.

Now let us consider the effect of the acoustic attenuation of the constitutive materials in the case of a longitudinal acoustic wave propagating along the superlattice growth axis z. In a medium with acoustic attenuation, the relation between the stress T and the strain $\partial u/\partial z$ is given by[26] $T=c(\partial u/\partial z)+\eta(\partial^2 u/\partial z\partial t)$, instead of $T=c(\partial u/\partial z)$ in a perfect elastic medium. Here c,η are the appropriate component of the elastic and viscosity tensor, respectively. This leads to the equation of wave propagation in each medium

$$\rho_\mu \frac{\partial^2 u}{\partial t^2}=c_\mu \frac{\partial^2 u}{\partial z^2}+\eta \frac{\partial^3 u}{\partial z^2 \partial t} \tag{3}$$

with $\mu=1,2$ referring to the two different layers. The solution is similar to that in perfect elastic media[19] except that the wave vector in each medium is now replaced by a complex number $K_\mu=k_\mu+i\alpha_\mu$, with $k_\mu=\omega/v_\mu$ ($v_\mu=\sqrt{c_\mu/\rho_\mu}$), $\alpha_\mu=\eta_\mu\omega^2/2\rho_\mu v_\mu^3$ (assuming $\alpha_\mu \ll k_\mu$ or $\omega\eta_\mu \ll c_\mu$). The phonon wave vector in the superlattice becomes also a complex number ($K=k+i\alpha$) and the dispersion relation turns out to be

$$\begin{aligned}
\cosh\alpha D\cos kD+i\sinh\alpha D\sin kD=&\left[\cos k_1d_1\cos k_2d_2-\frac{1}{2}\left[Z+\frac{1}{Z}\right]\sin k_1d_1\sin k_2d_2\right]\cosh\alpha_1d_1\cosh\alpha_2d_2\\
&+\left[-\sin k_1d_1\sin k_2d_2+\frac{1}{2}\left[Z+\frac{1}{Z}\right]\cos k_1d_1\cos k_2d_2\right]\sinh\alpha_1d_1\sinh\alpha_2d_2\\
&+i\left[\sin k_1d_1\cos k_2d_2+\frac{1}{2}\left[Z+\frac{1}{Z}\right]\cos k_1d_1\sin k_2d_2\right]\sinh\alpha_1d_1\cosh\alpha_2d_2\\
&+i\left[\cos k_1d_1\sin k_2d_2+\frac{1}{2}\left[Z+\frac{1}{Z}\right]\sin k_1d_1\cos k_2d_2\right]\cosh\alpha_1d_1\sinh\alpha_2d_2\ .
\end{aligned} \tag{4}$$

For $\alpha_1=\alpha_2=0$, one finds again Eq. (2) corresponding to lossless media.

The dispersion curve (ω-k) and the α-ω relation obtained by numerical resolution of Eq. (4) are drawn, respectively, in Figs. 2(a) and 2(b) for a $Si/Si_{0.5}Ge_{0.5}$ superlattice ($d_1=d_2=140$ Å) and compared to the ones calculated without acoustic attenuation. The coefficients of attenuation of Si and $Si_{0.5}Ge_{0.5}$ are apparently unreported in the literature, as well as their exact variation law as a function of the acoustic frequency. It is generally considered that the acoustic attenuation is proportional to ω^γ with $1<\gamma<2$, depending on the frequency range.[14,27] We have assumed that the acoustic attenuation in alloys is stronger than in pure crystals because of the disorder of substitution. We have thus taken almost arbitrarily $\alpha_1=0$ for Si and $\alpha_2=a\omega^2$ for $Si_{0.5}Ge_{0.5}$ (a is a constant). In any case, the general features of the acoustic attenuation effects discussed in the following are independent of this choice of the parameters α_1 and α_2.

From Fig. 2 we see that in the case without attenuation ($\alpha_1=\alpha_2=0$), the dispersion curve displays gaps at $k=n\pi/D$ ($n=1,2,3,\ldots$). The imaginary part of the wave vector is different from zero only at these gaps and the larger the gap, the higher the acoustic attenuation. When the acoustic attenuation of the constitutive materials is considered, the feature of the dispersion curve is changed [Fig. 2(a)]. The "gaps" seems to disappear at high frequency and at the place of the "gaps" there is only a continuous change of slope. At low frequency, as the acoustic attenuation is small, the slope change is abrupt and the dispersion curve is scarcely different from the one obtained by neglecting the acoustic attenuation. As to the imaginary part α of the wave vector, it increases with the frequency and still displays peaks at $k=n\pi/D$ [Fig. 2(b)], but the peaks are less conspicuous and even almost disappear when the attenuation of the constitutive materials is very strong. The disappearance of the gaps and the attenuation peaks for high-frequency phonons has been evidenced by phonon-transmission spectroscopy,[24] in which the expected transmission minima corresponding to the "gaps" at high frequency have not been observed.

Figure 3 shows the folded dispersion curves measured from the $Si/Si_{0.5}Ge_{0.5}$ superlattice sample with scattering wave vector q near the first-Brillouin-zone edge. The excited phonon modes correspond to wave vectors in the vicinity of $k\approx\pm\pi/D$ (LA and FLA_{-1} branches) and $k\approx\pm3\pi/D$ (FLA_{+1} and FLA_{-2}). Because of the important acoustic mismatch between Si and $Si_{0.5}Ge_{0.5}$, the energy gaps are sufficiently large to be detected by light scattering experiments, contrary to GaAs/AlAs superlattices. As the sample has $d_1=d_2$, the mode with even folding orders are very weak,[4,22] so we can only observe three modes (LA and $FLA_{\pm1}$) at low frequencies. The measured frequencies of the lowest two modes (LA and FLA_{-1}) agree very well with the calculation obtained by neglecting acoustic attenuation (solid and dashed lines) and the gap (~1 cm^{-1}) is clearly evidenced. A precise

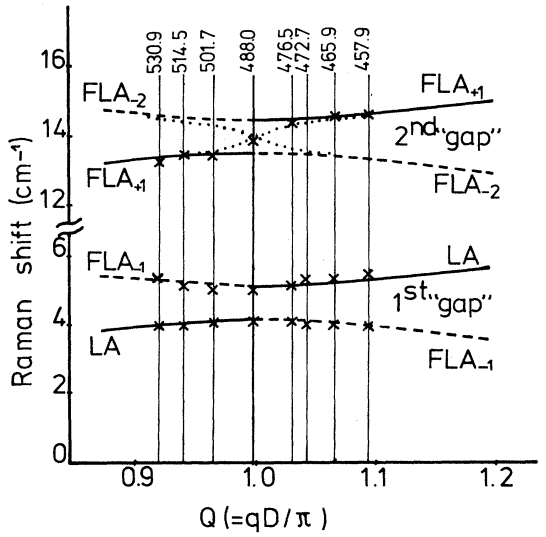

FIG. 3. Frequencies of the excited phonon modes as a function of the reduced scattering wave vector Q from both sides of the Brillouin-zone edge ($Q=1$) for the Si-$Si_{0.5}Ge_{0.5}$ superlattice ($d_1=d_2=140$ Å). Calculated values are drawn by solid or dashed lines in the case without acoustic attenuation, or by dotted lines in the case where the acoustic attenuation is considered. The crosses refer to experimental points. One finds that the acoustic attenuation can only be neglected for low frequencies ($\omega<6\ \mathrm{cm}^{-1}$).

measurement of this lowest-energy gap has been previously reported by Brugger.[8] As to the third mode which corresponds to the dispersion curve near $k=3\pi/D$, however, the frequency increases continuously with the wave vector and no abrupt change at the Brillouin-zone edge is observed. This can be well explained by the dispersion curve calculated here above, taking into account the acoustic attenuation which increases with the phonon frequency [inset of Fig. 2(a) and dotted line in Fig. 3].

It should be pointed out that although acoustic waves are strongly attenuated in the superlattice layers at this frequency region ($\sim 14\ \mathrm{cm}^{-1}$), their propagating distance can still cover several superlattice unit cells. It clearly appears that the phonon phase coherence in several superlattice unit cells is sufficient to give rise to folded acoustic modes in the Raman spectra. The existence of the "forbidden gaps" in superlattices constituted by acoustically lossless materials is due to the fact that the phonon density of states, which is proportional to $dk/d\omega$, is zero in the gaps. The presence of the acoustic attenuation of the constitutive layers changes the feature of the dispersion curve and increases significantly the phonon density of states, thus allowing the observation of the phonon modes in the "gap" through their coupling with light.

III. BROADENING OF THE PHONON MODES BY ACOUSTIC ATTENUATION AND OPTICAL ABSORPTION

The propagation of the acoustic wave in the superlattice produces periodic variation of strain. In the presence of the incident electromagnetic field, the photoelastic effect leads to a polarization which can be written as

$$P(z,t)=pSe^{i(kz-\omega t)}Ee^{i(k_i z-\omega_i t)}, \tag{5}$$

where p is the photoelastic constant; $S(E)$, $k(k_i)$, and $\omega(\omega_i)$ are, respectively, the amplitude, the wave vector, and the frequency of the strain (or the electric field of the incident light beam). This polarization acts as the source of the scattered light whose frequency is different to that of the incident light. By solving the Maxwell's equations one can find that the scattered electric field (anti-Stokes component) outside the superlattice for backward scattering can be expressed by[22]

$$E_s=A\frac{e^{iN(k+k_i-k_s)D}-1}{e^{i(k+k_i-k_s)D}-1}, \tag{6}$$

where k_s is the wave vector of the scattered light in the superlattice, N is the number of superlattice unit cells, and A is an amplitude factor which depends on the phonon frequency and on the structure of the superlattice.

When the acoustic attenuation is considered, the phonon wave vector k in Eq. (6) has to be replaced by the complex wave vector $k+i\alpha$. Then in the limit $N\to\infty$ (infinite superlattice), the intensity of the scattered light is given by

$$I_s=|E_s|^2=\frac{|A|^2}{\sin^2\frac{(k-q)D}{2}+\sinh^2\frac{\alpha D}{2}}, \tag{7}$$

where $q=k_s-k_i$ is the scattering wave vector. As the frequency of the scattered light is very close to that of the incident light, we can take $k_i\approx -k_s$ in the case of backward scattering. Then we have $q\approx 2k_s$.

The factor $|A|^2$ in expression (7) gives the intensity envelope function of the spectra, while the denominator of expression (7) determines the positions and widths of the phonon modes. One can obtain from Eq. (7) the wave-vector selection rule

$$k=q+\frac{2m\pi}{D}\quad (m=0,\pm1,\pm2,\dots). \tag{8}$$

The frequencies of the phonon modes are then determined by Eq. (8) and the dispersion relation (2) or (4). The tolerance of selected wave vectors Δk (full width at half maximum of I_s) is equal to 2α (for $\alpha D\ll 1$). The corresponding frequency linewidth of the phonon modes is then given by

$$\Delta\omega_{ac}=2\alpha\frac{d\omega}{dk}=2\alpha V_g, \tag{9}$$

where V_g is the group velocity of the phonons, i.e., the slope of the dispersion curve. For scattering wave vectors far from the Brillouin-zone boundaries, the dispersion curve is approximately linear and the line shape $I_s(\omega)$ of the phonon modes is Lorentzian.

As the linewidth due to the acoustic attenuation is proportional to α, it increases with the phonon frequency

and at low frequency the broadening is very small. In fact, as the semiconductors are usually opaque for excitation laser wavelength, the linewidth of the phonon modes at low frequency is mainly due to the optical absorption. In this case the wave vectors of the light in the two layers of the superlattice are complex numbers and the dispersion relation of optical wave in the superlattice is formally the same as that of acoustic wave [Eq. (4)], i.e,

$$\begin{aligned}\cosh\alpha_i D\cos k_i D + i\sinh\alpha_i D\sin k_i D = &\left[\cos k_{i1}d_1\cos k_{i2}d_2 - \frac{1}{2}\left[R+\frac{1}{R}\right]\sin k_{i1}d_1\sin k_{i2}d_2\right]\cosh\alpha_{i1}d_1\cosh\alpha_{i2}d_2 \\ &+\left[-\sin k_{i1}d_1\sin k_{i2}d_2 + \frac{1}{2}\left[R+\frac{1}{R}\right]\cos k_{i1}d_1\cos k_{i2}d_2\right]\sinh\alpha_{i1}d_1\sinh\alpha_{i2}d_2 \\ &+i\left[\sin k_{i1}d_1\cos k_{i2}d_2 + \frac{1}{2}\left[R+\frac{1}{R}\right]\cos k_{i1}d_1\sin k_{i2}d_2\right]\sinh\alpha_{i1}d_1\cosh\alpha_{i2}d_2 \\ &+i\left[\cos k_{i1}d_1\sin k_{i2}d_2 + \frac{1}{2}\left[R+\frac{1}{R}\right]\sin k_{i1}d_1\cos k_{i2}d_2\right]\cosh\alpha_{i1}d_1\sinh\alpha_{i2}d_2 \qquad (10)\end{aligned}$$

with $R=k_{i2}/k_{i1}$. Here $k_{i\mu}$ and $\alpha_{i\mu}$ are, respectively, the wave vector and absorption coefficient of the incident light in the two media of the superlattice ($\mu=1,2$); k_i,α_i are the ones corresponding to the superlattice. The wave vectors of the incident and scattered light k_i, k_s in Eq. (6) should then be replaced by complex numbers $k_i+i\alpha_i, k_s+i\alpha_s$. By neglecting the difference between α_s and α_i ($\alpha_s\approx\alpha_i=\alpha_{\rm op}$), we obtain the intensity of the scattered light

$$I_s=\frac{|A|^2}{\sin^2\frac{(k-q)D}{2}+\sinh^2\alpha_{\rm op}D}\ . \qquad (11)$$

The broadening due to optical absorption (FWHM) is then given, assuming $\alpha_{\rm op}D\ll 1$, by

$$\Delta\omega_{\rm op}\approx 4\alpha_{\rm op}\frac{d\omega}{dk}=4\alpha_{\rm op}V_g \qquad (12)$$

and the line shape is also approximately Lorentzian for scattering wave vector away from the Brillouin-zone edges.

The linewidth thus derived [Eqs. (9) and (12)] for phonon modes in superlattices is similar to the one deduced for the Brillouin line in homogeneous bulk media by Love[28] and by Sandercock.[29] But contrary to the case of homogeneous media where the phonon group velocity V_g is equal to the phase velocity and is k independent in the probed frequency range (the scattering wave vector is much smaller than the Brillouin zone of bulk crystals), V_g in superlattices undergoes strong variation versus k in the vicinity of Brillouin-zone edges and also depends on the considered phonon branch. Besides, the coefficient of acoustic attenuation α and optical absorption $\alpha_{\rm op}$ in superlattice, as well as the wave vectors k,k_i, are related to those in constitutive media by the complex dispersion relations [Eqs. (4) and (10)]. Only for wave vectors far from the Brillouin-zone boundaries can the coefficient of acoustic attenuation (optical absorption) in the superlattice be approximated by the average of those in the two media.

At low frequencies the phonon dispersion curve in superlattices presents gaps at the Brillouin-zone edge and near the gaps the dispersion curve flattens [see Fig. 2(a)], which means that the group velocity of the phonons becomes very small. As the linewidth is proportional to the group velocity [Eq. (12)], it should decrease when the wave vector of the phonon mode approaches the Brillouin-zone edge. This is a particular feature of the phonon linewidth in superlattices which has been confirmed by our experiments.

Figure 4 shows the spectra of the $Si/Si_{0.5}Ge_{0.5}$ superlattice with different wavelengths of laser excitation corresponding to scattering wave vectors at both sides of the first-Brillouin-zone edge ($Q\approx 1$). Let us focus on the upper mode of the first doublet whose frequency is around 5 cm^{-1}. This mode corresponds to FLA_{-1} for $Q<1$ and to LA for $Q>1$. Its intensity variation is quite remarkable. For small values of Q this line is weak with respect to the Brillouin line, but it grows rapidly for increasing value of Q in the first Brillouin zone and becomes much more intense than the Brillouin line near $Q=1$. This behavior does not depend on the nature of the constitutive layers and has been carefully analyzed in the case of GaAs/AlAs superlattices.[16,22]

Let us now examine the linewidth variation of this well-defined mode at about 5 cm^{-1}. This linewidth decreases from 0.72 cm^{-1} to 0.52 cm^{-1} with increasing values of Q in the range $0.92<Q<1$, though the optical absorption increases in this range (since the probing laser wavelength varies from 530.9 to 488 nm). This variation of linewidths can not be explained otherwise than by the flattening of the FLA branches near $Q=1$ which decreases $d\omega/dk$. For $Q>1$, the variation of $d\omega/dk$, the increase of the optical absorption, and the decrease of the experimental resolution all contribute to the increase of the linewidth (from 0.52 cm^{-1} at $Q=1$ to 0.93 cm^{-1} at $Q=1.09$). As to the highest-frequency mode in Fig. 4

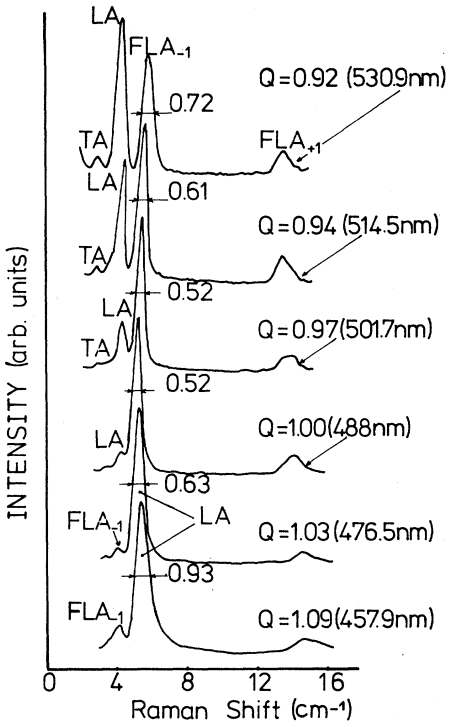

FIG. 4. Spectra of the same sample as in Fig. 3 with different excitation laser wavelengths. A double-grating spectrometer was used and the slit width was kept at 50 μm, corresponding to a resolution of about 0.5 cm^{-1} (varying slightly with laser wavelength). For low-frequency modes, the linewidth displays a minimum at $Q=1$ due to the flatness of the dispersion curve.

which corresponds to FLA_{+1}, the linewidth is very large because of the strong acoustic attenuation at this frequency and the disappearance of the gap in the dispersion curve.

It should be noted that the variation of the thickness or of the composition of the superlattice layers could also contribute to the broadening of the phonon modes. Such inhomogeneities can occur in the directions either parallel or perpendicular to the layers. From Raman scattering and x-ray diffraction measurements on different points of the sample, we have confirmed that the broadening induced by such defects is negligible with respect to that induced by optical and acoustical damping, in good-quality superlattices. Similar results have been reported previously.[14] To perform a systematical study of the influence of these defects, one should create them intentionally during the superlattice growth. This is out of the scope of this paper.

Finally it is worth pointing out that in the case where the optical absorption and acoustic attenuation are negligible (for example, for low-frequency phonon modes excited by red or infrared laser wavelengths) the Raman peaks are broadened by the limitation of the superlattice thickness. From Eq. (6) one can obtain the intensity expression for this case

$$I=|A|^2\frac{\sin^2[N(k-q)D]/2}{\sin^2[(k-q)D]/2} \tag{13}$$

which leads to a linewidth $\Delta\omega=2\pi V_g/ND$, ND being the total thickness of the superlattice. One can notice that this linewidth is also proportional to the group velocity of the phonon modes and can be the dominant cause of broadening in the case of too-thin superlattices.

IV. OPTICAL-ABSORPTION EFFECT ON THE RELATIVE INTENSITIES OF THE PHONON MODES

The intensities of the folded acoustic modes in the superlattices are related to the interference of the light waves scattered by different unit cells. We know that the wave vector of the polarization produced by the photoelastic effects is $k+k_i$ [see Eq. (5)]. From the wave-vector selection rule [Eq. (8)], we find that the phase difference $\Delta\Phi$ between the scattered light and the polarization after propagating one superlattice period D is $\Delta\Phi=k_sD-(k+k_i)D=2m\pi$, which means that the scattered electromagnetic field created by the polarization in two successive unit cells are coherently constructive. This can also be seen from Eq. (6) which, in the condition of Eq. (8) and in the absence of optical absorption and acoustic attenuation, becomes $E_s=NA$. This means that for the excited phonon modes, the amplitude of the scattered field is N times the one scattered from one unit cell. So the relative intensities of the phonon modes are totally determined by the factor $|A|^2$.

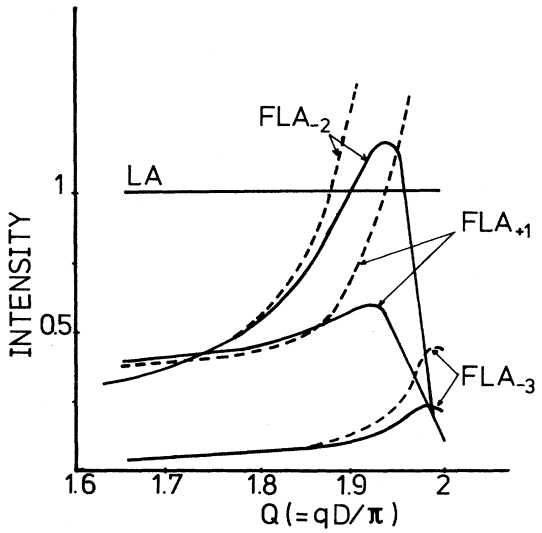

FIG. 5. Calculated intensities of the phonon modes for a GaAs/AlAs superlattice ($d_1=167$ Å, $d_2=458$ Å). The intensity of the Brillouin (LA) mode is normalized to 1. We have used (Refs. 30–32) n_1(GaAs)=4.215, n_2(AlAs)=3.287 for the real parts of the refractive indexes. The imaginary parts are taken $n_1'=0.378$, $n_2'=6.8\times10^{-4}$ for the case with optical absorption (solid line) and $n_1'=n_2'=0$ for the case without absorption (dashed line). The ratio of the Pockel's photoelastic constants of GaAs and AlAs is taken as 0.32 according to Ref. 16.

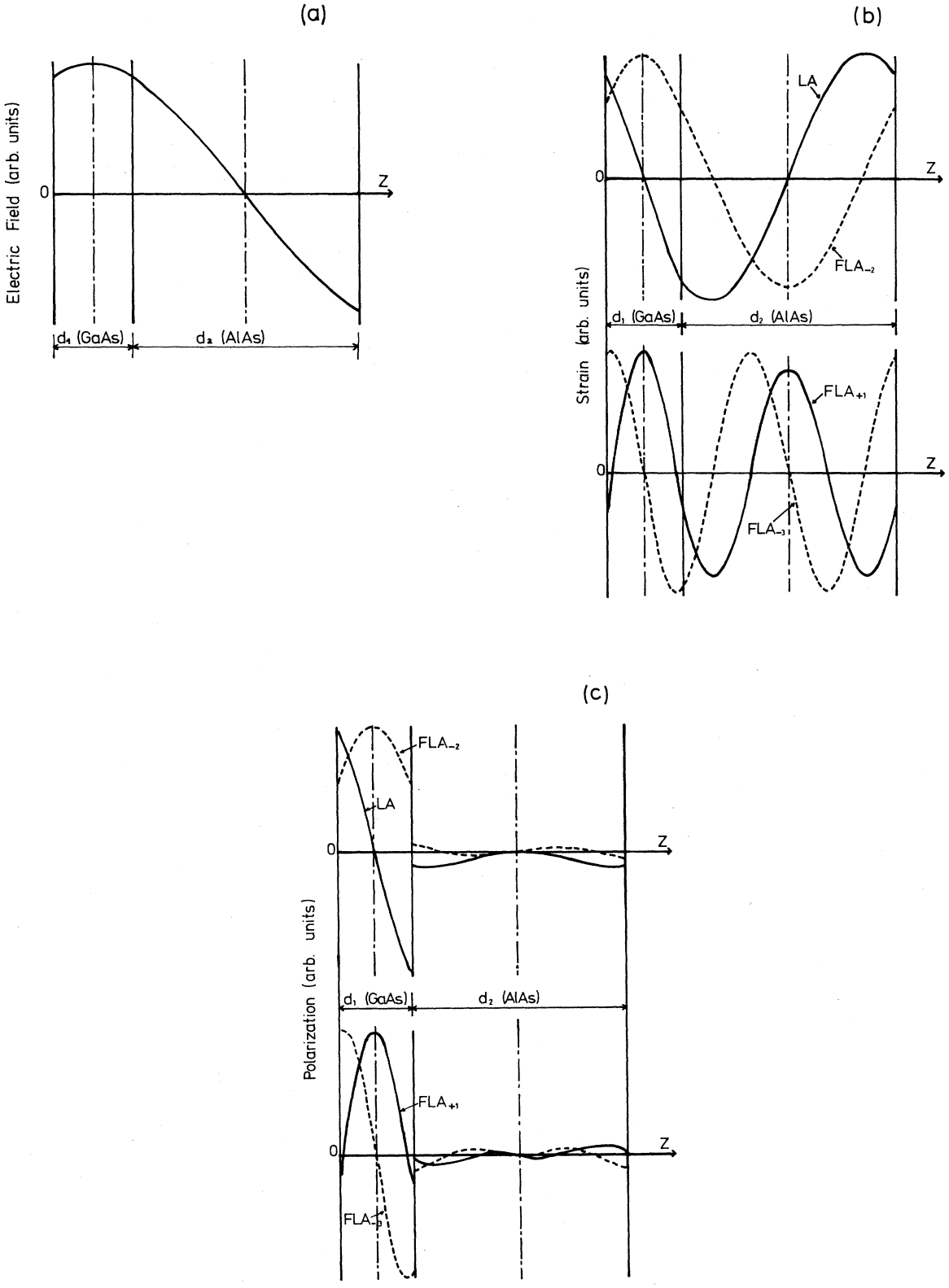

FIG. 6. Distribution along the z axis of the incident electromagnetic field (a), the strain corresponding to different phonon modes (b), and the corresponding polarizations in the GaAs/AlAs superlattice unit cell ($d_1 = 167$ Å, $d_2 = 458$ Å), calculated for Q at the second-Brillouin-zone edge. Here the optical absorption is not taken into account.

The factor $|A|^2$ is a complex function which depends on the constitutive material characteristics and the structure of the superlattice unit cell. In Ref. 22 the relative intensities have been calculated by taking into account the modulation of the photoelastic, acoustic, and optical properties in the superlattice, but the optical absorption has been neglected. Indeed, for excitation laser wavelength far from satisfying the Bragg condition, the optical damping only diminishes the effective number N of the superlattice unit cells and the relative intensities of the phonon modes are little affected. Therefore, a good agreement between the theory and experiments has been obtained for a wide range of scattering wave vectors not too close to the Brillouin-zone boundaries.[16] However, one can expect a significant effect of the optical absorption on the relative intensities for scattering wave vectors near Brillouin-zone boundaries which correspond to $Q=qD/\pi=2,4,6,\ldots$. Figure 5 shows the intensity calculated with (solid lines) or without (dashed lines) optical absorption for a GaAs/AlAs superlattice ($d_1=167$ Å, $d_2=458$ Å) for a scattering wave vector near the second-Brillouin-zone edge ($Q\approx 2$). The results with the consideration of the optical absorption are obtained by the same calculation as in Ref. 22, except that the wave vectors of the light waves are replaced by complex numbers. In Fig. 5 we see that the difference between the two cases becomes very important for $Q>1.85$. When Q is very close to 2, the intensities of the folded modes with respect to the Brillouin line are much reduced by the optical absorption.

This effect of the optical absorption can be understood schematically. Let us first consider the case of infinite superlattices without optical absorption. As we have discussed here above, the light scattered in different unit cells are constructive. It is therefore sufficient to consider the intensity of the light scattered in one unit cell. When the scattering wave vector tends to $2\pi/D$, the Bragg reflection for the incident light occurs. For an arbitrary unit cell of an infinite superlattice, the two semi-infinite superlattices at its both sides can be equivalent to two high-reflectivity mirrors which constitute a Fabry-Pérot resonator. The light is then bounced back and forth within the optical cavity and the effective interaction length of the light beam with the phonons in the unit cell is greatly increased. This will greatly enhance the intensities of the phonon modes.

The intensity enhancement at $Q\approx 2$ is different for different modes. To understand this, one can consider the distribution of the polarization corresponding to different modes in a superlattice unit cell. Qualitatively, if one neglects the reflection of the scattered waves at the superlattice interfaces, the intensity of the scattered light received by a detector outside the superlattice can be taken as be proportional to the square of the integration of the polarization amplitude in the volume of a unit cell, similar to the case of homogeneous media.[33] For $Q\approx 2$, the incident electromagnetic wave and the excited phonon modes (except for the lowest mode FLA_{-1} whose wavelength is much longer than the superlattice period and which is not considered here) correspond to stationary waves. From the expressions given in Ref. 22 [Eqs. (13) and (23)], one can find that all the wave functions are either symmetric or antisymmetric with regard to the central plane of each layer. Consequently, the polarization produced by the photoelastic effect, which is proportional to the product of the incident electric field and the strain field, is also symmetric or antisymmetric. Figure 6 shows the distribution of the incident electric field, the strain corresponding to different phonon modes, and the polarization in a superlattice unit cell along its growth axis for Q at the second-Brillouin-zone edge. If the polarization is symmetric, the scattered electromagnetic waves produced in the two halves of the layer will be constructive. Contrarily, if the polarization is antisymmetric, the light wave scattered in the layer will be self-compensated and its contribution to the intensity of the scattered light will be zero. The symmetry of the polarization is different in the two different kinds of layers. For a GaAs/AlAs superlattice, the symmetry in the GaAs layer is determinant for the intensity of the scattered light since its photoelastic constant is much larger than that of AlAs. If the polarization is antisymmetric in the GaAs layers, the intensity of the scattered light will be very weak. This is the case for the Brillouin mode of our sample. Therefore, when Q approaches 2, the intensity of the folded modes with respect to the Brillouin mode increase greatly.

When the superlattice is optically absorbing, there is no more symmetry (or antisymmetry) of the incident light field with regard to the central planes of the layers. This leads to the loss of the symmetry of the polarization. Besides, the resonant "cavity" effect of the superlattice is also much reduced since the light wave will be totally attenuated after propagating several rounds in the "cavity." Therefore, the optical absorption results in the reduction of the intensities of the folded modes with

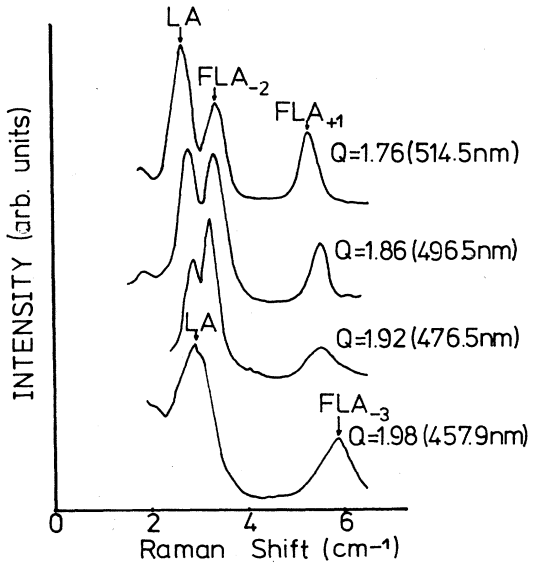

FIG. 7. Raman spectra of the same sample as in Fig. 5 with scattering wave vectors near the second-Brillouin-zone edge ($Q\approx 2$).

respect to the Brillouin mode, as shown in Fig. 5.

In Fig. 7 are reported the Raman spectra of this sample with scattering wave vectors near the second-Brillouin-zone edge. We see that when q approaches $2\pi/D$, the intensity of the FLA_{-2} mode begins by increasing and becomes stronger than the LA mode for $Q=1.92$. Then when Q approaches further to the Brillouin-zone edge ($Q=1.98$), the LA mode becomes again dominant. Besides, though the two modes (FLA_{+1} and FLA_{-3}) of the second doublet are not separated experimentally, an abnormally important shift of the peak towards high frequency is observed at $Q=1.98$ which may be attributed to the intensity decrease of the FLA_{+1} mode with respect to the FLA_{-3} mode. All these features agree qualitatively with the calculation when the optical absorption is taken into account (see Fig. 5).

V. CONCLUSION

This study is complementary to previous ones[16,22] in which the alternating layers of the superlattice were considered as lossless media. In the present paper we have studied both theoretically and experimentally the effect of acoustic attenuation and optical absorption on the Raman scattering by superlattice acoustic phonons propagating normally to the layers. At low frequency where the acoustic attenuation is small, a reduction of the linewidth at the Brillouin-zone edge is observed due to the flatness of the phonon dispersion curve in this region. At high frequency, due to the strong acoustic attenuation, the translational symmetry D along the growth axis is partially lost and as a consequence, the phonon dispersion curve displays no more feature of gaps at the Brillouin-zone edges. The optical absorption of the superlattice is found not only to broaden the phonon peak linewidth, but also to affect the relative intensities for scattering wave vectors near the second-Brillouin-zone edge.

ACKNOWLEDGMENTS

We would like to thank H. Brugger for helpful discussions and for the supply of the $Si/Si_{0.5}Ge_{0.5}$ superlattice.

[1]For a recent review paper, see, J. Sapriel, in *Proceedings of the SPIE,* edited by O. J. Glembocki, F. H. Pollak, and F. Ponce (SPIE, Bellingham, 1988), Vol. 946, p. 136.
[2]L. Colvard, R. Merlin, M. V. Klein, and A. C. Gossard, Phys. Rev. Lett. **45**, 298 (1980).
[3]J. Sapriel, J. C. Michel, J. C. Toledano, R. Vacher, J. Kervarec, and R. Regreny, Phys. Rev. B **28**, 2007 (1983).
[4]C. Colvard, T. A. Gant, M. V. Klein, R. Merlin, R. Fisher, H. Morkoç, and A. C. Gossard, Phys. Rev. B **31**, 2080 (1985).
[5]B. Jusserand, F. Alexandre, J. Dubard, and D. Paquet, Phys. Rev. B **33**, 2897 (1986).
[6]J. Sapriel, J. Chavignon, F. Alexandre, and R. Azoulay, Phys. Rev. B **33**, 7118 (1986).
[7]H. Brugger, G. Abstreiter, H. Jorke, H. J. Herzog, and E. Kasper, Phys. Rev. B **33**, 5928 (1986).
[8]H. Brugger, H. Reiner, G. Abstreiter, H. Jorke, H. J. Herzog, and E. Kasper, Superlatt. Microstruct. **2**, 451 (1986).
[9]J. Sapriel, J. He, J. Chavignon, F. Alexandre, R. Azoulay, G. Le Roux, J. Burgeat, and R. Vacher, in *Proceedings of the European Materials Research Society, Strasbourg, 1986,* edited by P. A. Glasow, Y. I. Nissim, J.-P. Noblanc, and J. Speight (Les Editions de Physique, Paris, 1986), and references therein.
[10]D. J. Lockwood, M. W. C. Dharma-Wardana, J. M. Baribeau, and D. C. Houghton, Phys. Rev. B **35**, 2243 (1987).
[11]B. Jusserand, D. Paquet, F. Mollot, F. Alexandre, and G. Le Roux, Phys. Rev. B **35**, 2808 (1987).
[12]G. P. Schwartz, G. J. Gualtieri, W. A. Sunder, and L. A. Farrow, Phys. Rev. B **36**, 4868 (1987).
[13]D. Levy, S.-L. Zhang, M. V. Klein, J. Klem, and H. Morkoç, Phys. Rev. B **36**, 8032 (1987).
[14]P. V. Santos and L. Ley, Phys. Rev. B **36**, 3325 (1987).
[15]P. V. Santos, A. K. Sood, M. Cardona, K. Ploog, Y. Ohmori, and H. Okamoto, Phys. Rev. B **37**, 6381 (1988).
[16]J. Sapriel, J. He, B. Djafari-Rouhani, R. Azoulay, and F. Mollot, Phys. Rev. B **37**, 4099 (1988).
[17]J. He, J. Sapriel, R. Azoulay, G. Le Roux, and H. Brugger, in *Proceedings of the SPIE,* edited by F. Capasso, G. H. Döhler, and J. N. Schulman (SPIE, Bellingham, 1988), Vol. 943, p. 192.
[18]J. He, J. Sapriel and H. Brugger, Phys. Rev. B **39**, 5919 (1989).
[19]S. M. Rytov, Akust. Zh. **2**, 71 (1956) [Sov. Phys.—Acoust. **2**, 68 (1956)].
[20]J. Sapriel, B. Djafari-Rouhani, and L. Dobrzynski, Surf. Sci. **126**, 197 (1983).
[21]A. S. Barker, Jr., J. L. Mertz, and A. C. Gossard, Phys. Rev. B **17**, 3181 (1978).
[22]J. He, B. Djafari-Rouhani, and J. Sapriel, Phys. Rev. B **37**, 4086 (1988).
[23]V. Narayanamurti, H. L. Störmer, M. A. Chin, A. C. Gossard, and W. Wiegmann, Phys. Rev. Lett. **43**, 2012 (1979).
[24]P. V. Santos, L. Ley, J. Mebert, and O. Koblinger, Phys. Rev. B **36**, 1306 (1987).
[25]S. Tamura, D. C. Hurley, and J. P. Wolfe, Phys. Rev. B **38**, 1427 (1988).
[26]R. M. Christenson, *Theory of Viscoelasticity* (Academic, New York, 1971), p. 7.
[27]D. A. Pinnow, IEEE J. Quantum Electron. **QE-6**, 223 (1970).
[28]W. F. Love, Phys. Rev. Lett. **31**, 822 (1973).
[29]J. R. Sandercock, Phys. Rev. Lett. **28**, 237 (1972).
[30]D. E. Aspnes and A. A. Studna, Phys. Rev. B **27**, 985 (1983).
[31]S. Adachi, J. Appl. Phys. **58**, R1 (1985).
[32]W. Michael Yim, J. Appl. Phys. **42**, 2854 (1971).
[33]W. Hayes and R. Loudon, *Scattering of Light by Crystals* (Wiley, New York, 1978).